Broadband coupler between silicon waveguide and hybrid plasmonic waveguide

Yi Song, Jing Wang, Qiang Li, Min Yan, and Min Qiu*

Laboratory of Photonics and Microwave Engineering, School of Information and Communication Technology, Royal Institute of Technology, Electrum 229, 164 40 Kista, Sweden

**min@kth.se*

Abstract: Efficient broadband coupling of light between a dielectric waveguide and a hybrid plasmonic waveguide is investigated theoretically. A plasmonic linear taper is used as a coupler which connects the two types of waveguides. Broadband coupling is realized by such a compact plasmonic taper with a length of only 0.4μm, which achieves a coupling efficiency of 70% (1.5dB) at the 1.55μm telecommunication wavelength.

OCIS codes: (240.6680) Surface plasmons; (250.5403) Plasmonics.

References and links

1. S. A. Maier, P. E. Barclay, T. J. Johnson, M. D. Friedman, and O. Painter, "Low-loss fiber accessible plasmon waveguide for planar energy guiding and sensing," Appl. Phys. Lett. **84**(20), 3990 (2004).
2. S. A. Maier, P. G. Kik, H. A. Atwater, S. Meltzer, E. Harel, B. E. Koel, and A. A. G. Requicha, "Local detection of electromagnetic energy transport below the diffraction limit in metal nanoparticle plasmon waveguides," Nat. Mater. **2**(4), 229–232 (2003).
3. R. Charbonneau, N. Lahoud, G. Mattiussi, and P. Berini, "Demonstration of integrated optics elements based on long-ranging surface plasmon polaritons," Opt. Express **13**(3), 977–984 (2005).
4. J. Takahara, S. Yamagishi, H. Taki, A. Morimoto, and T. Kobayashi, "Guiding of a one-dimensional optical beam with nanometer diameter," Opt. Lett. **22**(7), 475–477 (1997).
5. S. I. Bozhevolnyi, V. S. Volkov, E. Devaux, J.-Y. Laluet, and T. W. Ebbesen, "Channel plasmon subwavelength waveguide components including interferometers and ring resonators," Nature **440**(7083), 508–511 (2006).
6. D. F. P. Pile, T. Ogawa, D. K. Gramotnev, T. Okamoto, M. Haraguchi, M. Fukui, and S. Matsuo, "Theoretical and experimental investigation of strongly localized plasmons on triangular metal wedges for subwavelength waveguiding," Appl. Phys. Lett. **87**(6), 061106 (2005).
7. M. Yan, and M. Qiu, "Guided plasmon polariton at 2D metal corners," J. Opt. Soc. Am. B **24**(9), 2333–2342 (2007).
8. L. Chen, J. Shakya, and M. Lipson, "Subwavelength confinement in an integrated metal slot waveguide on silicon," Opt. Lett. **31**(14), 2133–2135 (2006).
9. M. Z. Alam, J. Meier, J. S. Aitchison, and M. Mojahedi, "Super mode propagation in low index medium," in Conference on Lasers and Electro-Optics/Quantum Electronics and Laser Science Conference and Photonic Applications Systems Technologies, OSA Technical Digest Series (CD) (Optical Society of America, 2007), paper JThD112.
10. R. F. Oulton, V. J. Sorger, D. A. Genov, D. F. P. Pile, and X. Zhang, "A hybrid plasmonic waveguide for subwavelength confinement and long-range propagation," Nat. Photonics **2**(8), 496–500 (2008).
11. R. F. Oulton, G. Bartal, D. F. P. Pile, and X. Zhang, "Confinement and propagation characteristics of subwavelength plasmonic modes," N. J. Phys. **10**(10), 105018 (2008).
12. R. Slavador, and A. Martinez, "C. G-Meca, R. Ortuno, J. Marti, "Analysis of hybrid dielectric plasmonic waveguides," IEEE J. Quantum Electron. **14**, 1496–1501 (2008).
13. D. Dai, and S. He, "A silicon-based hybrid plasmonic waveguide with a metal cap for a nano-scale light confinement," Opt. Express **17**(19), 16646–16653 (2009).
14. G. Veronis, and S. Fan, "Theoretical investigation of compact couplers between dielectric slab waveguides and two-dimensional metal-dielectric-metal plasmonic waveguides," Opt. Express **15**(3), 1211–1221 (2007).
15. N. N. Feng, and L. Dal Negro, "Plasmon mode transformation in modulated-index metal-dielectric slot waveguides," Opt. Lett. **32**(21), 3086–3088 (2007).
16. P. Ginzburg, D. Arbel, and M. Orenstein, "Gap plasmon polariton structure for very efficient microscale-to-nanoscale interfacing," Opt. Lett. **31**(22), 3288–3290 (2006).
17. R. Yang, M. A. Abushagur, and Z. Lu, "Efficiently squeezing near infrared light into a 21 nm-by-24 nm nanospot," Opt. Express **16**(24), 20142–20148 (2008).
18. J. Tian, S. Q. Yu, W. Yan, and M. Qiu, "Broadband high-efficiency surface-plasmon-polariton coupler with silicon-metal interface," Appl. Phys. Lett. **95**(1), 013504 (2009).
19. Z. Han, A. Y. Elezzabi, and V. Van, "Experimental realization of subwavelength plasmonic slot waveguides on a silicon platform," Opt. Lett. **35**(4), 502–504 (2010).

#127157 - $15.00 USD Received 16 Apr 2010; revised 27 May 2010; accepted 1 Jun 2010; published 3 Jun 2010

20. S. Sederberg, V. Van, and A. Y. Elezzabi, "Monolithic integration of plasmonic waveguides into a complimentary metal-oxide-semiconductor- and photonic-compatible platform," Appl. Phys. Lett. **96**(12), 121101 (2010).
21. X. Guo, M. Qiu, J. M. Bao, B. J. Wiley, Q. Yang, X. N. Zhang, Y. G. Ma, H. K. Yu, and L. M. Tong, "Direct coupling of plasmonic and photonic nanowires for hybrid nanophotonic components and circuits," Nano Lett. **9**(12), 4515–4519 (2009).
22. E. D. Palik, "Handbook of Optical Constants of Solids," (Academic Press, New York, 1998).

1. Introduction

There exists great expectation for integrated photonic circuits, which would not only speed up on-chip information processing but also promise many other photonics-related applications. Plasmonic waveguides, with a capability to guide optical signals in deep subwavelength scale, have the promise to be an ideal candidate for the next-generation highly-integrated photonic circuitry. Several different types of plasmonic waveguides have been proposed, such as metallic nanoparticle chain waveguides [1,2], metallic wires or stripe waveguides [3,4], channel or wedge plasmonic waveguides [5–7], plasmonic slot waveguides [8], hybrid plasmonic waveguides [9–13]. In general, these plasmonic waveguides have a trade-off between their mode confinement and propagation length. Among them, the hybrid plasmonic (HP) waveguide [9–13] is found to be relatively superior: it has a large propagation length (several-hundred micrometers) with a subwavelength mode confinement. Although superior compared to other types of plasmonic waveguides, the propagation length of a hybrid plasmonic waveguide [9–13] is still far too short compared to those of conventional dielectric waveguides (typically a few centimeters). In view of this, plasmonic waveguides are likely to be the key waveguiding component for miniaturized devices, while dielectric waveguides would remains useful for delivering optical signals over a relatively long span. Hybrid integration of plasmonic and dielectric waveguides can probably provide the best compromise between compactness and low loss. In view of this, efficient coupling between a dielectric waveguide and a plasmonic waveguide is a vital problem which needs to be addressed carefully.

Several methods [8,14–21] have been proposed for achieving efficient coupling between dielectric waveguides and various plasmonic waveguides. For plasmonic slot (metal-dielectric-metal) waveguides, several different coupling schemes have been demonstrated both theoretically [14–17] and experimentally [8,18–20]. Recently, there was also an experimental demonstration of the coupling between a silicon waveguide and a dielectric loaded plasmonic waveguide through a long silicon taper [20]. Efficient directional coupling between dielectric nanowires and plasmonic nanowires has also been demonstrated experimentally [21]. However, so far no coupling scheme for hybrid plasmonic waveguides has been investigated. In this paper, the efficient coupling between a dielectric silicon waveguide and a hybrid plasmonic waveguide will be investigated in detail. A linear plasmonic taper connecting the two types of waveguides is deployed for achieving efficient light coupling. Our design fully takes experimental considerations including both material and geometry into account, therefore is ready realizable.

2. Silicon and plasmonic waveguides

The silicon waveguide studied here is a standard silicon on insulator (SOI) waveguide with a height h_{Si} = 250nm and a width w_{Si} = 450nm. With these geometrical parameters, only a fundamental transverse electric (TE) mode and a fundamental transverse magnetic (TM) mode (Fig. 1(b)) are supported at λ = 1550nm. By depositing an alumina layer (of thickness h_{Al2O3} = 50nm) and then a silver layer (of thickness h_{Ag} = 100nm) on top of the SOI waveguide (Fig. 1(c)), a hybrid plasmonic waveguide is obtained. When the width w_{plas} is smaller than 240nm, only a single TM mode exists in the HP waveguide at λ = 1550nm. At a width of w_{plas} = 200nm, the E_y mode field of the HP waveguide is shown in Fig. 1(d). The E_y field cut along the x = 0 vertical line (Fig. 1(d)) reveals further details of the mode: the electric field is largely concentrated within the 50nm alumina layer. All modes in Fig. 1 are obtained by the finite element method (FEM) based commercial software COMSOL Multiphysics. The parameters

#127157 - $15.00 USD Received 16 Apr 2010; revised 27 May 2010; accepted 1 Jun 2010; published 3 Jun 2010

of the materials are set to be n_{Si} = 3.45, n_{SiO2} = 1.45, n_{Al2O3} = 1.74, and the dispersive permittivity ε_{Ag} is calculated according to a Drude model which is fitted with the experiment data [22].

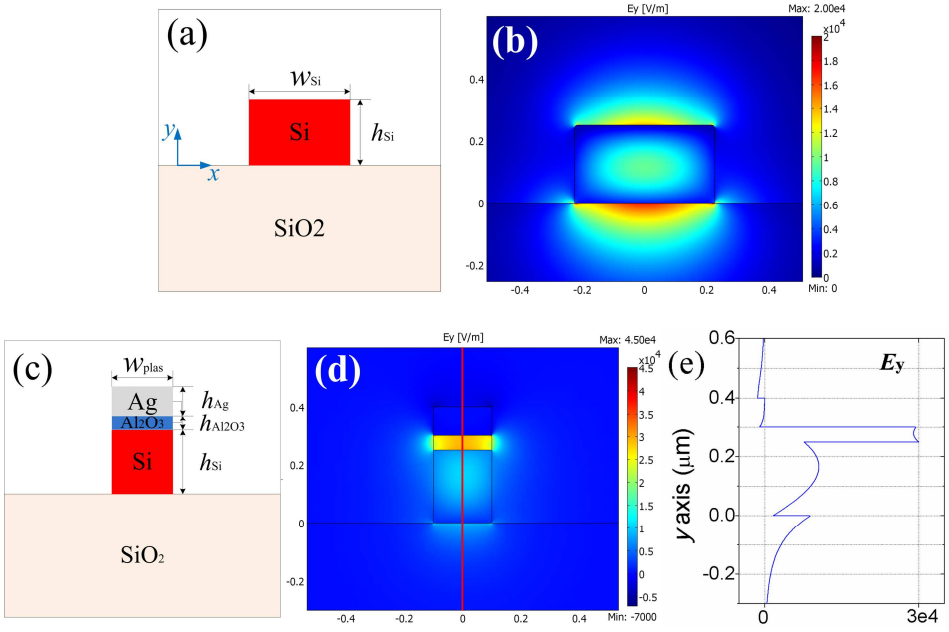

Fig. 1. (a) The cross-section of a SOI waveguide with the width w_{Si} and height h_{Si}. (b) The field distribution E_y of the fundamental TM mode for the same SOI waveguide. (c) The cross-section of a HP waveguide composed by depositing an alumina layer (h_{Al2O3}) and then a silver layer (h_{Ag}) on top of a SOI waveguide with a height h_{Si} and width w_{plas}. (d) The field distribution E_y of the fundamental TM mode for a HP waveguide with the width w_{Si} = 450nm and h_{Si} = 250nm, h_{Al2O3} = 50nm, h_{Ag} = 100nm. (e) The cross-section of E_y at x = 0 (red solid line in (d)) for the same HP waveguide.

3. Coupler

A three dimensional finite-difference time-domain (FDTD) method is used to simulate the light coupling performance between the silicon waveguide (Fig. 1(a)) and the HP waveguide (Fig. 1(c)). Material parameters are the same as those used in the FEM calculations. The fundamental TM mode of the silicon waveguide is excited by a Gaussian source with a central wavelength λ_0 = 1550nm, at which ε_{Ag} = −87-8.7i [22].

Firstly, the coupling by directly connecting the Si waveguide and the HP waveguide is investigated (Fig. 2(a)). Figure 2(b) shows the E_y field distributions at different cross sections for such a direct coupling. There is an obvious enhancement of E_y field as the light transmits into the HP waveguide from the Si waveguide.

In this simple scenario, the coupling loss is mainly caused by two factors, the interface reflection and the mismatch between the two waveguide modes. Our FDTD simulations reveal that the interface reflection for such a direct coupling is less than 4%. Therefore the radiation loss caused by the mode mismatch determines the total coupling efficiency. It can be expected that, as the width of the HP waveguide decreases, the coupling efficiency will decrease due to the increase in their mode mismatch. Figure 2(c) shows the coupling efficiency (λ = 1550nm) from the Si waveguide to the HP waveguide as the width of the HP waveguide varies. At w_{plas} = 450nm, the coupling efficiency is η = 85% (0.7dB), while at w_{plas} = 100nm η decreases rapidly to 45% (3.4dB). As a reference, the portion of the power flow in the central section of the silicon waveguide, corresponding to the area of the HP waveguide, is also shown in Fig. 2(c). The power portion in the central section of the Si waveguide is found only comparable to

#127157 - $15.00 USD Received 16 Apr 2010; revised 27 May 2010; accepted 1 Jun 2010; published 3 Jun 2010

the coupling efficiency between the Si and the HP waveguide when the HP waveguide width is larger than 250nm. For a narrow HP waveguide (w_{plas}<250nm), the actual coupling efficiency is larger than the portion of the power flowing in the central section of the Si waveguide. This suggests that a narrow HP waveguide can collect light from a dielectric waveguide with a much larger cross-sectional area with a moderate efficiency. In order to obtain an even higher coupling efficiency, especially from a Si waveguide to a HP waveguide with a very narrow width (<250nm), direct connection of the two waveguides is certainly not sufficient. More specifically, when directly coupling light from a Si waveguide with w_{Si} = 450nm to a HP waveguide with w_{plas} = 200nm, the coupling efficiency is only η = 60% (2.2dB).

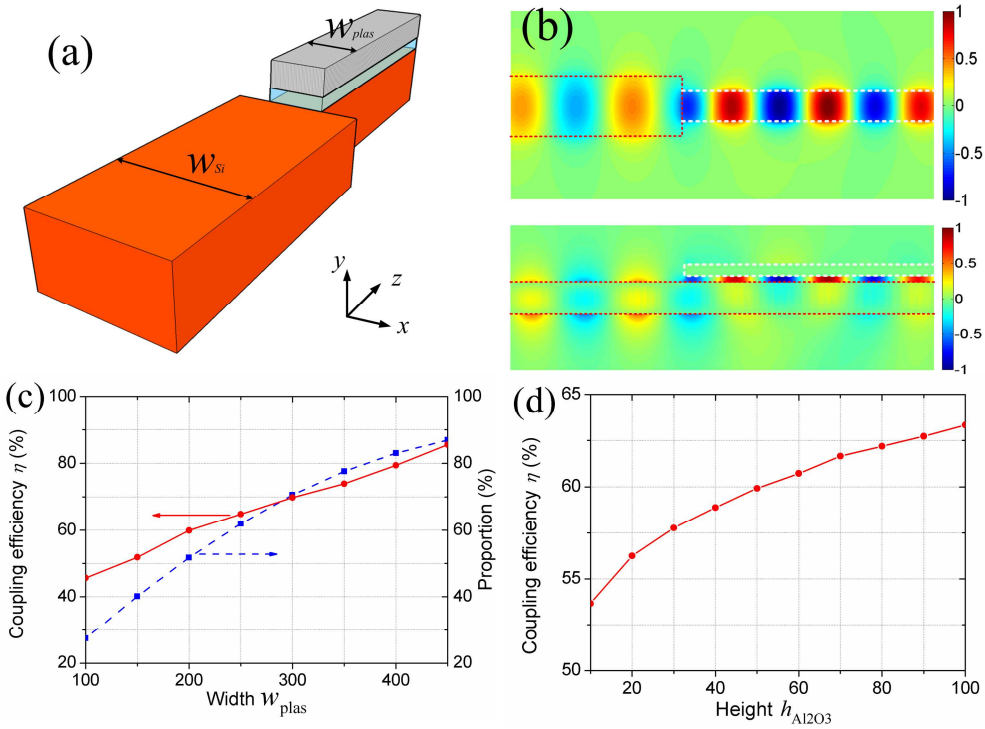

Fig. 2. (a) Schematic diagram for the direct coupling. (b) E_y field distributions for the direct coupling between a silicon waveguide with a width w_{Si} = 450nm and a hybrid plasmonic waveguide with a width w_{plas} = 200nm, in the plane of y = 275nm (the center plane of the alumina layer, top) and the plane of x = 0 (bottom). (c) The coupling efficiency shown as a function of the HP waveguide width (red solid line), compared with the proportion of power flow in the central section of the silicon waveguide with the same width (blue dashed line). (d) The coupling efficiency shown as a function of the height of the alumina layer.

In passing, we show the dependence of the direct coupling efficiency η on the height of the alumina layer h_{Al2O3} in Fig. 2(d) for HP waveguide with fixed width w_{plas} = 200nm . As the alumina layer becomes larger, more power will be guided in the Si layer. This is expected, since a thicker alumina layer reduces the mode mismatch between these two waveguides and therefore increases the coupling efficiency. However the increase in efficiency is not significant: when the height of the alumina layer h_{Al2O3} increases from 10nm to 100nm, the coupling efficiency η increases from 53% to 63%. Considering that an increase in h_{Al2O3} leads to a larger HP mode field, we limit the height of the alumina layer h_{Al2O3}<100nm to ensure a relatively good mode field confinement together with a relatively long propagation length.

In the following, we introduce a hybrid plasmonic linear taper to enhance the coupling efficiency between a silicon waveguide (w_{Si} = 450nm) and a HP waveguide (w_{plas} = 200nm,

#127157 - $15.00 USD Received 16 Apr 2010; revised 27 May 2010; accepted 1 Jun 2010; published 3 Jun 2010

h_{Al2O3} = 50nm) (see Fig. 3 (a)). The taper has the same structure as the HP waveguide in the vertical (y) direction, and the width decreases linearly from 450nm to 200nm. A taper eliminates the abrupt change in geometry (and partially in material parameters). Therefore it is expected to reduce the radiation loss. For a linear plasmonic taper, the taper slope is vital for coupling efficiency: a sufficiently long taper can be expected to reduce the radiation loss to the minimum and increase the coupling efficiency to be as high as the direct coupling with a 450nm HP waveguide (~85%). However, on the other hand, we have to consider the propagation loss which is an inherent property for any plasmonic waveguide. The existence of propagation loss certainly prevents the deployment of a very long HP taper. It is one of our objectives in this paper to identify an optimal taper length for achieving the highest coupling efficiency between the waveguides.

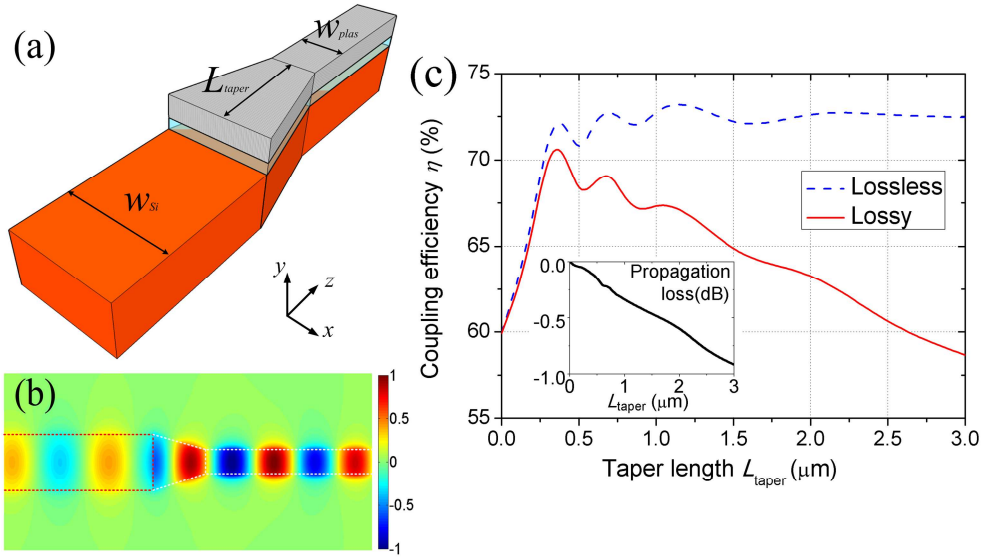

Fig. 3. (a) Schematic diagram for the HP-taper coupler. (b) E_y distribution at in the plane of y = 275nm (the center plane of the alumina layer) for the coupling with a 0.4μm-long HP taper. (c) The coupling efficiency of the HP taper as a function of its length (red solid line), compared with the same design with lossless silver (blue dashed line). The inset shows the corresponding propagation loss for the HP taper.

Again through 3D FDTD simulations, we obtain the dependence of the coupling efficiency on the taper length L_{taper} at the wavelength λ = 1550nm, shown in Fig. 3(c) (the red solid line). As the taper length L_{taper} increases from 0 to 0.4μm, the coupling efficiency η increases rapidly from 60% (2.2dB) to 70% (1.5dB). This reflects that even a very short HP taper will improve significantly the coupling efficiency. When the taper length further increases, the propagation loss becomes larger and starts to deteriorate the total coupling efficiency. Indeed, ignoring the weak oscillation caused by the Fabry-Perot effect of the HP taper, we observe that the coupling efficiency keeps decreasing as the taper length L_{taper} increases from 0.4 to 3μm. For a taper length of 3μm, the coupling efficiency is only 58% (2.3dB), even lower than that for the direct coupling. Hence for practical purpose, it is better to limit the taper length L_{taper} to be smaller than 2.5μm.

It is known that the coupling loss is dominated by the radiation loss and the propagation loss. The interface reflection for the HP taper accounts for only <2% in energy loss from our 3D FDTD simulation, therefore it can be safely neglected. In our previous discussions, the trade-off between the radiation and propagation losses has been studied. To see the contribution by each factor more clearly, we further carry out 3D FDTD calculations for the same structures but with lossless silver. The corresponding coupling efficiency at λ = 1550nm

#127157 - $15.00 USD Received 16 Apr 2010; revised 27 May 2010; accepted 1 Jun 2010; published 3 Jun 2010

is also shown in Fig. 3(c) (the blue dashed line). With lossless material, the energy loss in the coupling is solely due to the radiation loss. From Fig. 3(c), again by ignoring the oscillations in the curve, we see that as the taper length increases from 0 to 3μm, the coupling efficiency keeps increasing to be ~72% (1.4dB). For a taper length larger than 0.4μm, the reduction of radiation loss as the increase of the taper length is not so obvious compared with shorter tapers. By relating the coupling efficiency with the previously obtained coupling efficiency with lossy silver, we obtain the propagation loss for the HP taper, which is shown in the inset of Fig. 3. The inset shows the almost linear increase of the propagation loss when the taper length increases. At a taper length of 3μm, the propagation loss is as large as 0.9dB which well explains the low coupling efficiency. For a 0.4μm-long HP taper (Fig. 3(b)), the relatively low radiation loss (1.4dB) and low propagation loss (0.1dB) make it the optimal coupler with the highest coupling efficiency. As a tapered coupler without relying on any resonance mechanism, a broadband enhancement in coupling efficiency can be anticipated. In Fig. 4, we explicitly show the coupling efficiency of the optimal HP coupler (0.4μm long) over a broad-band wavelength range. Compared with the direct coupling, a 0.5~0.7dB improvement in coupling efficiency is obtained for the HP taper over the wavelength range of 1450~1650nm.

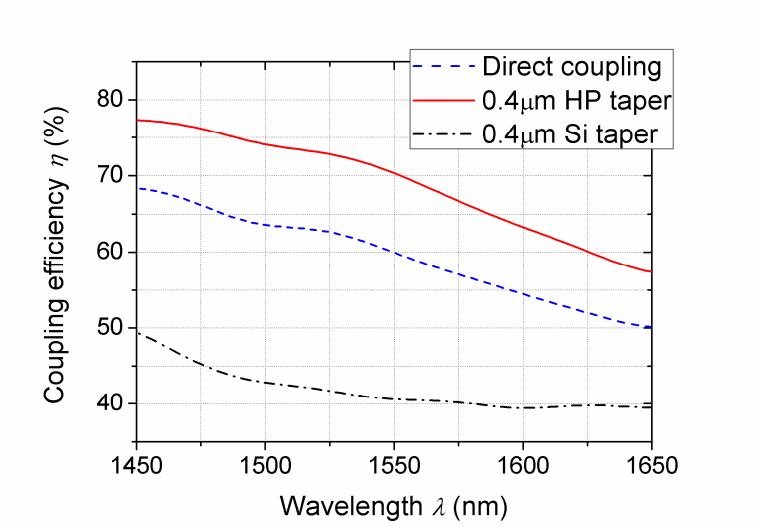

Fig. 4. Coupling efficiency in the wavelength range 1450~1650nm, for the direct coupling (blue dashed line), coupling through a 0.4μm-long HP taper (red solid line) and a 0.4μm-long silicon taper (black dash-dotted line).

As a further comparison, the coupler composed by a 0.4μm-long silicon taper, which has the similar structure as the HP taper but with the alumina and silver layers removed, is also examined by the 3D FDTD simulation. A very low coupling efficiency of ~41% (3.9dB) is obtained at the wavelength 1550nm (Fig. 4, the black dash-dotted line), which is caused by the drastic mode mismatch between a 200nm silicon waveguide and a 200nm HP waveguide.

4. Conclusions

In conclusion, a highly-efficient, broadband, and compact coupling between a standard SOI waveguide (450 × 250nm) and a narrow hybrid plasmonic waveguide (200nm wide) is achieved with a 0.4μm-long hybrid plasmonic linear taper at 1550nm wavelength. Compared with a direct coupling, the coupling efficiency is enhanced from ~60% (2.2dB) to ~70% (1.5dB). The designed coupler can facilitate an efficient interchange of optical signals between a dielectric waveguide and a plasmonic waveguide. Such a hybrid integration can take advantages of both the low-loss nature of silicon waveguides and the sub-wavelength

#127157 - $15.00 USD Received 16 Apr 2010; revised 27 May 2010; accepted 1 Jun 2010; published 3 Jun 2010

nature of plasmonic waveguides. Our coupler proposal therefore has potential applications in near-future nanophotonic systems.

Acknowledgements

This work is supported by the Swedish Foundation for Strategic Research (SSF) and the Swedish Research Council (VR).

#127157 - $15.00 USD Received 16 Apr 2010; revised 27 May 2010; accepted 1 Jun 2010; published 3 Jun 2010